Generalized n-Photon Resonant $2n$-Wave Mixing in an $(n+1)$-Level System with Phase-Conjugate Geometry

Zhanchun Zuo,[1] Jiang Sun,[2] Xia Liu,[1] Qian Jiang,[1] Guangsheng Fu,[2] Ling-An Wu,[1] and Panming Fu[1,*]

[1]*Laboratory of Optical Physics, Beijing National Laboratory for Condensed Matter Physics, Institute of Physics, Chinese Academy of Sciences, Beijing 100080, China*

[2]*Department of Physics, Hebei University, Hebei 071002, China*

(Received 8 May 2006; published 8 November 2006)

A generalized scheme for phase-conjugate resonant $2n$-wave mixing, which has a high efficiency and is easy for phase matching, is proposed. As a new type of coherent laser spectroscopy this approach can be employed for studying highly excited atomic states or states with a high angular momentum. To demonstrate its feasibility we have studied the doubly excited autoionizing Rydberg states of Ba by phase-conjugate six-wave mixing, and have furthermore achieved eight-wave mixing in Na. This method may find wide application in related areas such as coherent transient spectroscopy, Autler-Townes spectroscopy and electromagnetically induced transparency. In particular, it may provide new insights into the nature of highly excited states.

DOI: 10.1103/PhysRevLett.97.193904 PACS numbers: 42.65.−k, 32.80.Rm, 42.50.Hz

The physics of wave-mixing interactions has been a subject of intense research activity for the past few decades. Various types of nonlinear spectroscopy based on wave mixing are capable of addressing dynamic information related to the structure of matter because the nonlinear susceptibility exhibits resonances at the natural frequencies of the medium [1]. Recently, various resonance-enhanced nondegenerate four-wave mixing (FWM) schemes have been developed by our group [2–5]. For example, Rayleigh-type nondegenerate FWM [4], which can be employed for the measurement of ultrafast longitudinal relaxation time in the frequency domain, has been demonstrated. We have also studied a new type of two-photon resonant FWM in a dressed atomic system [5]. This process provides a spectroscopic tool for measuring not only the resonant frequency and dephasing rate but also the transition dipole moment between two highly excited atomic states.

Higher-order wave-mixing effects have been observed in several experiments [6–10]. However, one of the difficulties encountered is that as the order of the nonlinearity increases, more complex beam geometries are usually required to satisfy the phase-matching conditions. Moreover, the nonlinear signal decreases by several orders of magnitude with an increase in the order of nonlinearity of the interaction. In this Letter we shall report for the first time a generalized scheme for resonant $2n$-wave mixing in $(n+1)$-level systems with phase-conjugate geometry. Similar to the corresponding nondegenerate FWM technique we developed, the phase-matching conditions are not so stringent and can be achieved over a very wide frequency range from many hundreds to thousands of cm^{-1} [4,5]. Moreover, due to the multiple resonance with the atomic transition frequencies, the $2n$-wave mixing signal will be enhanced tremendously.

Since this technique involves n-photon resonant excitation we can study highly excited states with high sensitivity by purely optical means. Here we shall investigate the doubly excited autoionizing Rydberg states of Ba by phase-conjugate six-wave mixing. Previously, these types of experiments were usually performed in atomic beams, where the resulting electrons or ions from the decay of autoionizing states were detected [11–15]. The methods used probed the populations of the autoionizing states. By contrast, resonant $2n$-wave mixing is a type of coherent laser spectroscopy, where coherence between the ground and autoionizing states is involved. As a result, it is possible to investigate dephasing of this coherence. We shall also demonstrate that even higher-order wave mixing can be observed easily by performing eight-wave mixing in sodium.

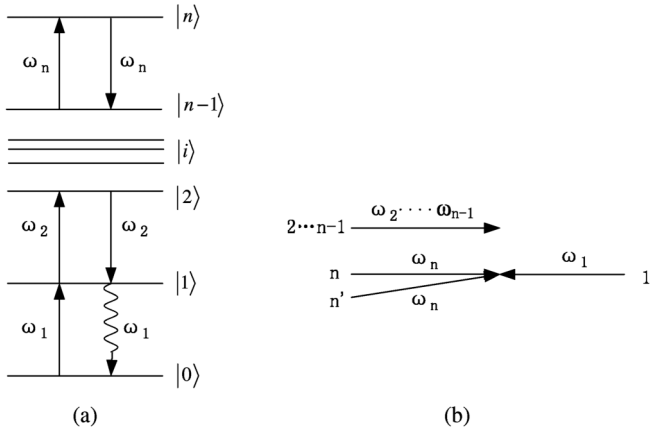

FIG. 1. (a) Energy-level diagram for resonant $2n$-wave mixing in an $(n+1)$-level system. (b) Schematic of phase-conjugate $2n$-wave mixing.

Let us consider a cascade $(n+1)$-level system [Fig. 1(a)], where states between $|i-1\rangle$ and $|i\rangle$ are coupled by a dipolar transition with resonant frequency Ω_i and dipole moment matrix element μ_i. As shown in Fig. 1(b), beams n and n' have the same frequency ω_n and a small angle exists between them. Beams 2, 3 to $n-1$ with frequencies ω_2, ω_3 to ω_{n-1}, respectively, propagate along the direction of beam n, while beam 1 with frequency ω_1 propagates along the opposite direction of beam n. Assume that $\omega_i \simeq \Omega_i$ so that ω_i drives the transition from $|i-1\rangle$ to $|i\rangle$. The simultaneous interactions of atoms with beams 1, 2 to n will induce atomic coherence between $|0\rangle$ and $|n\rangle$ through resonant n-photon transition. This n-photon coherence is then probed by beams n', $n-1$ to 2, and as a result a $2n$-wave mixing signal of frequency ω_1 is generated almost opposite to the direction of beam n'.

Let the detunings be represented by $\Delta_i = \Omega_i - \omega_i$, so after a canonical transformation the effective Hamiltonian is

$$H = \hbar\Delta_1|1\rangle\langle 1| + \hbar(\Delta_1+\Delta_2)|2\rangle\langle 2| + \cdots + \hbar(\Delta_1+\Delta_2+\cdots+\Delta_n)|n\rangle\langle n| - (\mu_1 E_1|1\rangle\langle 0| + \mu_2 E_2|2\rangle\langle 1| + \cdots + \mu_n E_n|n\rangle\langle n-1| + \text{H.c.}). \quad (1)$$

Here, $E_i = \varepsilon_i e^{i\mathbf{k}_i\cdot\mathbf{r}}$ $(i = 1 \text{ to } n-1)$ and $E_n = \varepsilon_n e^{i\mathbf{k}_n\cdot\mathbf{r}} + \varepsilon_n' e^{i\mathbf{k}_n'\cdot\mathbf{r}}$ are the complex incident laser fields; $\mathbf{k}_i$ and $\mathbf{k}_n'$ are the wave vectors of beams i and n', respectively. The nonlinear polarization responsible for the $2n$-wave mixing signal is proportional to the off-diagonal density matrix element ρ_{10}, which can be obtained from the density matrix equations with relaxation terms properly included

$$\frac{d\rho}{dt} = -\frac{i}{\hbar}[H,\rho] + \left(\frac{d\rho}{dt}\right)_{\text{relax}}. \quad (2)$$

Assuming that the incident fields are weak so that the perturbation theory is applicable, the $2n$-wave mixing can be described by the following perturbation chain: $\rho_{00}^{(0)} \to \rho_{10}^{(1)} \to \rho_{20}^{(2)} \to \cdots \to \rho_{n0}^{(n)} \to \cdots \to \rho_{20}^{(2n-2)} \to \rho_{10}^{(2n-1)}$. We obtain

$$\rho_{10}^{(2n-1)}(\mathbf{r}) = i\frac{(-1)^{n+1}G_1|G_2|^2\cdots|G_{n-1}|^2 G_n (G_n')^* \exp[i(\mathbf{k}_1+\mathbf{k}_n-\mathbf{k}_n')\cdot\mathbf{r}]}{(i\Delta_1+\Gamma_{10})^2[i(\Delta_1+\Delta_2)+\Gamma_{20}]^2\cdots[i(\Delta_1+\cdots+\Delta_{n-1})+\Gamma_{(n-1)0}]^2}\frac{1}{i(\Delta_1+\Delta_2+\cdots+\Delta_n)+\Gamma_{n0}}, \quad (3)$$

where $G_i = \mu_i\varepsilon_i/\hbar$ and $G_n' = \mu_n\varepsilon_n'/\hbar$ are the coupling coefficients; Γ_{i0} is the transverse relaxation rate between states $|i\rangle$ and $|0\rangle$. The $2n$-wave mixing signal intensity is proportional to $|\rho_{10}^{(2n-1)}(\mathbf{r})|^2$. According to Eq. (3), the transverse relaxation rate Γ_{n0} can be deduced if we scan ω_n while keeping ω_1 to ω_{n-1} fixed.

The peculiarity of this technique is that although $2n$-wave mixing involves $n+1$ incident beams with n different frequencies, the phase-matching condition depends only on beams 1, n, and n' with two frequencies ω_1 and ω_n involved. Specifically, according to Eq. (3) the $2n$-wave mixing signal propagates along the direction $\mathbf{k}_1+\mathbf{k}_n-\mathbf{k}_n'$. This can be understood from the viewpoint of energy and momentum conservation. As shown in Fig. 1(a), the frequency of the $2n$-wave mixing $\omega_s = \omega_1+\omega_2+\cdots+\omega_n-\omega_n-\omega_{n-1}-\cdots-\omega_2 = \omega_1$. Accordingly, the corresponding momentum terms are $\mathbf{k}_s = \mathbf{k}_1+\mathbf{k}_2+\cdots+\mathbf{k}_n-\mathbf{k}_n'-\mathbf{k}_{n-1}-\cdots-\mathbf{k}_2 = \mathbf{k}_1+\mathbf{k}_n-\mathbf{k}_n'$. It is worth mentioning that there also exists lower order wave mixing in the process. However, all these signals propagate along the direction $\mathbf{k}_1$ so they can be resolved spatially from the $2n$-wave mixing signal. For example, conservation of energy for the $2(n-1)$-wave mixing implies $\omega_s = \omega_1+\omega_2+\cdots+\omega_{n-1}-\omega_{n-1}-\omega_{n-2}-\cdots-\omega_2 = \omega_1$, thus we have $\mathbf{k}_s = \mathbf{k}_1+\mathbf{k}_2+\cdots+\mathbf{k}_{n-1}-\mathbf{k}_{n-1}-\mathbf{k}_{n-2}-\cdots-\mathbf{k}_2 = \mathbf{k}_1$.

We first set up an experiment to demonstrate four-photon resonant eight-wave mixing in Na, where the states $3S_{1/2}$ ($|0\rangle$), $3P_{1/2}$ ($|1\rangle$), $5S_{1/2}$ ($|2\rangle$), $3P_{3/2}$ ($|3\rangle$), and $4D$ ($|4\rangle$) form a folded five-level system [Fig. 2(a)]. Here, Na was chosen simply because of its convenient resonant frequencies. The Na vapor was contained in a stainless steel heat pipe at a temperature around 230 °C with an argon buffer gas pressure of 1 torr. Four dye lasers L1, L2, L3, and L4, which were pumped by the second harmonics of a Quanta-Ray Nd:YAG laser, had a linewidth of 0.007 nm and pulse width 5 ns. All the incident beams were linearly polarized in the same direction. They were focused to spots approximately 2.0 mm in diameter. The lasers L1, L2, and L3, which had wavelengths of 589.6, 615.4, and 616.1 nm, were used to drive the transitions from $3S_{1/2}$ to $3P_{1/2}$, from $3P_{1/2}$ to $5S_{1/2}$ and from $5S_{1/2}$ to $3P_{3/2}$, respectively. On the other hand, the laser L4 was split at the beam splitter into beams 4 and 4′, which then intersected in the

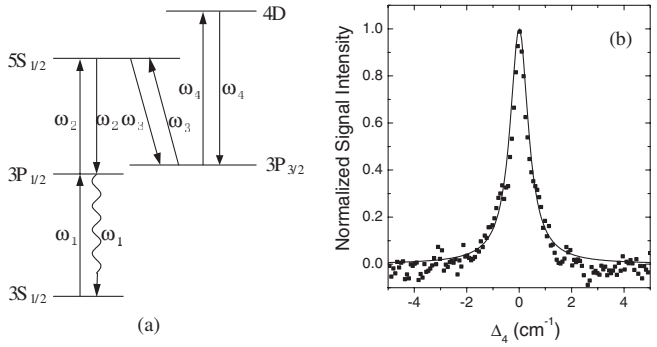

FIG. 2. (a) Energy-level diagram for four-photon resonant eight-wave mixing in Na. (b) Eight-wave mixing spectrum. The solid curve is the theoretical curve with $\Gamma_{30} = 0.4\ \text{cm}^{-1}$.

oven at a small angle of 0.5° to drive the transition from $3P_{3/2}$ to $4D$ (568.8 nm). To avoid strong absorption at the resonant frequency of the transition $3S_{1/2}$-$3P_{1/2}$, the wavelength of L1 was detuned from the exact resonance by 0.06 nm. Figure 2(b) presents the eight-wave mixing signal intensity as a function of Δ_4 when ω_1, ω_2, and ω_3 are on resonance. Here the energies of beams 1, 2, 3, 4, and $4'$ are 1 μJ, 0.05 mJ, 0.07 mJ, 0.12 mJ, and 0.07 mJ, respectively. Through theoretical fitting (solid curve) we obtain the dephasing rate $\Gamma_{30} = 0.4\ \mathrm{cm}^{-1}$, which is mainly due to the laser linewidths.

One important application of $2n$-wave mixing is that it can be employed as a spectroscopic tool to study highly excited atomic states with high sensitivity. In the following, we report six-wave mixing experiments in Ba, where the ground state $6s^2$ ($|0\rangle$), the intermediate state $6s6p$ ($|1\rangle$), the Rydberg state $6snd$ ($|2\rangle$) and the doubly excited autoionizing Rydberg state $6pn'd$ ($|3\rangle$) form a cascade four-level system. The Ba vapor was at a temperature around 660 °C with an argon buffer gas pressure of 1 torr. We first tuned the frequencies ω_1 and ω_2 to the resonances of the transitions $6s^2{}^1S_0$-$6s6p{}^1P_1$ (553.5 nm) and $6s6p{}^1P_1$-$6s17d{}^1D_2$ (427 nm), respectively, and scanned ω_3 over a wide frequency region with wavelengths from 442 to 463 nm. Here again the wavelength of L1 was detuned from exact resonance by 0.06 nm. The results presented in Fig. 3(a) show a series of resonant lines, which are independent of beam 2 of frequency ω_2. These lines originate from the two-photon resonant FWM in the $6s^2{}^1S_0$-$6s6p{}^1P_1$-$6snd$ ($6sns$) cascade three-level system with beams 1, 3, and $3'$ as incident beams. As we increased the sensitivity by increasing the incident laser intensities, including now beam 2, a very broad line accompanied by several asymmetric narrower lines appeared [lower curve in Fig. 3(b)]. Here the energies of beams 1, 2, 3, and $3'$ are 1 μJ, 0.06 mJ, 0.03 mJ, and 0.01 mJ, respectively. To verify that these lines were due to the six-wave mixing, we first fixed ω_3 and scanned ω_2. Figure 3(c) presents the result when ω_3 is fixed to the frequency shown by the arrow in Fig. 3(b). It exhibits a resonant line at a frequency corresponding to the transition from $6s6p{}^1P_1$ to $6s17d{}^1D_2$. We then performed dressed-atom two-photon resonant FWM [5] in the $6s^2{}^1S_0$-$6s6p{}^1P_1$-$6s17d{}^1D_2$ cascade three-level system with a strong coupling field of frequency ω_3 driving the transition $6s17d{}^1D_2$-$6p_{3/2}17d$. As demonstrated in Ref. [5], at exact two-photon resonance the presence of the coupling field suppresses the FWM signal. This can be seen from the upper curve in Fig. 3(b) which has a dip with a broad linewidth also. Comparing the two spectra in Fig. 3(b), we conclude that the broad line in the six-wave mixing spectrum (lower curve) manifests the autoionizing Rydberg state $6p_{3/2}17d$, where the line shape is broadened due to the depletion broadening of autoionizing states at high power [16]. On the other hand, the asymmetric narrow lines correspond to the transitions $6s17d{}^1D_2$-$6p_{3/2}nd$ with $n \neq 17$, as marked in the figure. It is worth mentioning

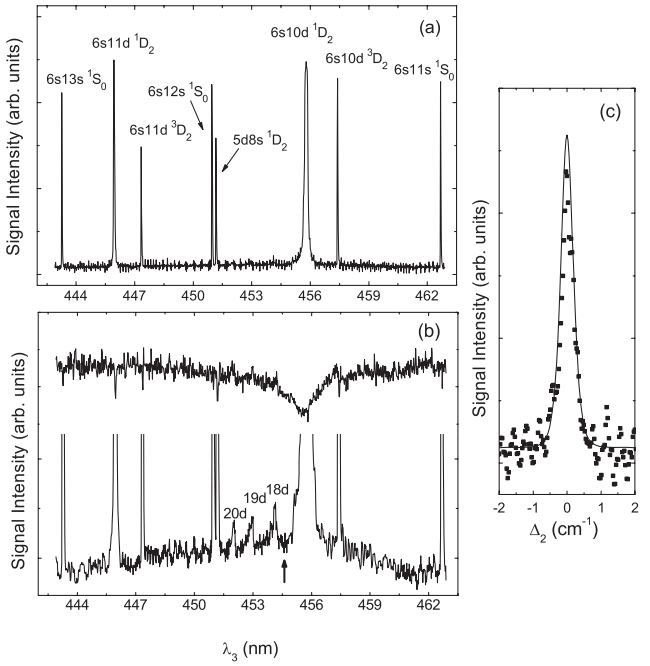

FIG. 3. (a) Four-wave mixing spectrum in the $6s^2$-$6s6p$-$6snd$ ($6sns$) cascade three-level system in Ba with beams 1, 3, and $3'$ as incident beams. (b) Lower curve: six-wave mixing spectrum in the $6s^2$-$6s6p$-$6s17d$-$6pnd$ cascade four-level system in Ba. Here the frequencies ω_1 and ω_2 were tuned to the resonances of the transitions $6s^2$-$6s6p$ (553.5 nm) and $6s6p$-$6s17d$ (427 nm), respectively, and ω_3 was scanned over a wide frequency region with wavelengths from 442 to 463 nm. The broad line manifests the autoionizing Rydberg state $6p_{3/2}17d$, while the asymmetric narrow lines correspond to the transitions $6s17d$-$6p_{3/2}nd$ with $n \neq 17$. Upper curve: FWM signal intensity versus the wavelength of the coupling field in dressed-atom two-photon resonant FWM with the coupling field driving the transition $6s17d$-$6p_{3/2}17d$. (c) Six-wave mixing signal as a function of Δ_2 when ω_3 is fixed to a frequency shown by the arrow in (b). Resonance occurs at a frequency corresponding to the transition $6s6p$-$6s17d$.

that, in the excitation of autoionizing states $6pnd$, the Rydberg outer electron is basically a spectator when the core electron is excited from $6s$ to $6p$. This is the isolated core excitation (ICE) [11]. However, for the third laser which has high intensity, the Rydberg electron is in fact affected by the excitation of the core electron through the electron-electron Coulomb repulsion. As a result, the outer electron can be left in a different quantum state, giving the narrow lines in the lower curve of Fig. 3(b). The asymmetry of these lines arises from the variations of spectral density of the autoionizing states and the overlap integral from the initial bound state [12].

As is well known, multistep ICE is an important technique for studying autoionizing Rydberg states. It is perhaps the best approach for producing the double Rydberg states of atoms [13], which is related to the basic three-body Coulomb problem. Also, dielectronic recombination, an important energy-loss mechanism in plasmas, can be

studied by this technique [14]. Recently, sudden ICE by femtosecond laser pulses has been employed for studying the evolution and decay of autoionizing states in the time domain [15]. Our experiment is the first demonstration of the application of multiwave mixing to ICE. In contrast to previous ICE experiments, where populations of autoionizing states are probed, resonant $2n$-wave mixing is a type of coherent laser spectroscopy, which involves coherence between the ground and autoionizing Rydberg states. As a result, it is possible to investigate dephasing of this coherence. Moreover, resonant $2n$-wave mixing can be performed in vapor cells so the effects of collision with buffer gases can be readily studied.

In addition to highly excited atomic states, another possible field of study is states with high angular momentum. This is because, due to the selection rule, states with angular momentum $L = n$ can be excited through n-photon resonant excitation if the ground state has $L = 0$. Our method also provides a new approach for other relevant fields. For example, we can extend our method to the time-domain region. As in the case of the relation between two-photon resonant FWM and the trilevel echo [3,17], it is possible to develop various types of echoes relevant to the n-photon resonant $2n$-wave mixing by employing a pulse sequence. Also, a new type of Autler-Townes spectroscopy can be developed if a strong coupling field is applied to drive the transition between $|n\rangle$ and an additional state $|n + 1\rangle$, so that the $2n$-wave mixing spectrum exhibits an Autler-Townes splitting [5]. This technique provides a spectroscopic tool for measuring the transition dipole moment between states $|n\rangle$ and $|n + 1\rangle$. Finally, if beam 2 of frequency ω_2 is a strong field, then our method is related to the electromagnetically induced transparency based wave mixing, which has attracted much attention in recent years [18].

Let us now consider the technical advantages of resonant $2n$-wave mixing. First, the technique is Doppler-free when the incident lasers have narrow bandwidths, because if ω_1 is within the Doppler profile of the transition from $|0\rangle$ to $|1\rangle$, then only atoms in a specific velocity group will contribute to the signal. Second, since the phase-conjugate geometry is adopted, phase matching can be achieved for a very wide frequency range, as shown in Figs. 3(a) and 3(b), and the optical alignment is relatively simple. Third, the generation of the wave mixing signal is very efficient because all the transitions are in resonance. Finally, compared to the method of detecting fluorescence from excited states [19], our scheme is still realizable even when states $|2\rangle$ to $|n\rangle$ have long radiative lifetimes so that direct detection of the fluorescence is difficult. This is because transitions between these states are driven by lasers, and so long as $|1\rangle$ to $|0\rangle$ is a strongly coupled transition, the wave-mixing signal can be emitted via this strong transition [see Fig. 1(a)].

In conclusion, we have proposed a generalized $2n$-wave mixing scheme, where a phase-matching geometry allows us to isolate higher-order wave mixing. As a new type of coherent laser spectroscopy this method provides information about the relaxation of high-order atomic coherence and so is particularly suitable for studying highly excited atomic states or states with high angular momentum.

The authors gratefully acknowledge financial support from the National Natural Science Foundation of China under Grants No. 10374113, 10574155, and 60578029, and from the National Program for Basic Research in China Grant No. 2001CB309301.

*Author to whom correspondence should be addressed.

[1] Y. R. Shen, *The Principles of Nonlinear Optics* (John Wiley & Sons, Inc., New York, 1984).
[2] Z. Yu, H. Lu, P. Ye, and P. Fu, Opt. Commun. **61**, 287 (1987); X. Mi, Z. Yu, Q. Jiang, and P. Fu, Phys. Rev. A **48**, 3203 (1993).
[3] P. Fu, Z. Yu, X. Mi, X. Li, and Q. Jiang, Phys. Rev. A **50**, 698 (1994); P. Fu, X. Mi, Z. Yu, Q. Jiang, Y. Zhang, and X. Li, Phys. Rev. A **52**, 4867 (1995); P. Fu, Y. Wang, Q. Jiang, X. Mi, and Z. Yu, J. Opt. Soc. Am. B **18**, 370 (2001).
[4] P. Fu, Q. Jiang, X. Mi, and Z. Yu, Phys. Rev. Lett. **88**, 113902 (2002); J. Sun, Q. Jiang, Z. Yu, X. Mi, and P. Fu, Opt. Commun. **223**, 187 (2003).
[5] J. Sun, Z. Zuo, X. Mi, Z. Yu, Q. Jiang, Y. Wang, L.-A. Wu, and P. Fu, Phys. Rev. A **70**, 053820 (2004).
[6] G. Gibson, T. S. Luk, A. McPherson, and C. K. Rhodes, Phys. Rev. A **43**, 371 (1991).
[7] R. Trebino and L. A. Rahn, Opt. Lett. **12**, 912 (1987).
[8] K. Tominaga and K. Yoshihara, Phys. Rev. Lett. **76**, 987 (1996).
[9] T. Steffen and K. Duppen, Phys. Rev. Lett. **76**, 1224 (1996).
[10] H. Kang, G. Hernandez, and Y. Zhu, Phys. Rev. Lett. **93**, 073601 (2004).
[11] W. E. Cooke, T. F. Gallagher, S. A. Edelstein, and R. M. Hill, Phys. Rev. Lett. **40**, 178 (1978); W. E. Cooke and T. F. Gallagher, Phys. Rev. Lett. **41**, 1648 (1978).
[12] N. H. Tran, R. Kachru, and T. F. Gallagher, Phys. Rev. A **26**, 3016 (1982); N. H. Tran, P. Pillet, R. Kachru, and T. F. Gallagher, Phys. Rev. A **29**, 2640 (1984).
[13] U. Eichmann, V. Lange, and W. Sandner, Phys. Rev. Lett. **68**, 21 (1992).
[14] V. Klimenko, L. Ko, and T. F. Gallagher, Phys. Rev. Lett. **83**, 3808 (1999); V. Klimenko and T. F. Gallagher, Phys. Rev. Lett. **85**, 3357 (2000).
[15] J. E. Thoma and R. R. Jones, Phys. Rev. Lett. **83**, 516 (1999); H. Maeda, W. Li, and T. F. Gallagher, Phys. Rev. Lett. **85**, 5078 (2000); J. G. Story and H. N. Ereifej, Phys. Rev. Lett. **86**, 612 (2001).
[16] W. E. Cooke, S. A. Bhatti, and C. L. Cromer, Opt. Lett. **7**, 69 (1982).
[17] T. W. Mossberg, R. Kachru, S. R. Hartmann, and A. M. Flusberg, Phys. Rev. A **20**, 1976 (1979).
[18] See, e.g., S. E. Harris, Phys. Today **50**, No. 7, 36 (1997).
[19] A. M. Lyyra, H. Wang, T.-J. Whang, W. C. Stwalley, and L. Li, Phys. Rev. Lett. **66**, 2724 (1991).